Short communication

Study of electrodeposited polypyrrole coatings for the corrosion protection of stainless steel bipolar plates for the PEM fuel cell

M.A. Lucio García [a], Mascha A. Smit [b],*

[a] CIE-UNAM, Priv. Xochicalco S/N, 62580 Temixco, Morelos, Mexico
[b] Unidad de Materiales, Centro de Investigación Científica de Yucatán (CICY), Calle 43 no. 130, col. Chuburná de Hidalgo, 97200 Mérida, Yucatán, Mexico

Abstract

Polypyrrole coatings were prepared on stainless steel SS304 in order to study the corrosion protection provided by the conductive polymer in a simulated PEM fuel cell environment. The polypyrrole was deposited by electrochemical polymerization with 0.04, 0.07 and 0.14 g cm^{-2} onto SS304 electrodes. Polarization curves, taken after immersion for 1, 3 or 24 h in 0.1 M sulphuric acid at either room temperature or 60 °C were used as an accelerated test. For short immersion times, it was found that corrosion current densities (at free corrosion potentials), diminished up to 2 orders of magnitude for samples tested at room temperature and up to 4 orders of magnitude for samples tested at 60 °C. Furthermore, at potentials in the range of the PEM fuel cell anode potential, corrosion rates also decreased up to several orders of magnitude. However, these protective properties were lost at longer times of immersion. The addition of DBSA to the polypyrrole coatings did lead to improved corrosion current densities at the free corrosion potential, however due to the loss of passivity of these samples, the corrosion rates in the potential range applicable to PEM fuel cells were either similar to or larger than bare metal. SEM was used to determine the morphology of the coatings and showed that the most homogeneous coating was obtained for 0.07 g cm^{-2} polypyrrole, without the incorporation of DBSA.
© 2005 Elsevier B.V. All rights reserved.

Keywords: PEM fuel cell; Bipolar plates; Polypyrrole; Corrosion; Stainless steel

1. Introduction

There is a vast amount of research going on into the different types of fuel cells in order to improve material performance, cell life time and decrease production costs. One of the obstacles to obtain these goals is formed by the bipolar plates. Bipolar plates for PEM fuel cells are conventionally made from compressed graphite, which is difficult to machine, making it a high volume and high cost part for PEM fuel cells. Therefore, there is extensive research into the development of new low-weight, low-cost materials for bipolar plates, which should have high electronic and thermal conductivity, impermeability for hydrogen, good compressive strength and high stability in the fuel cell environment. There are two main streams of development: the first are the conductive polymer composites, of which some commercial developments are already available, the second is formed by metals. A review of the different options and developments is given by Hermann [1]. In the case of the metallic bipolar plates, specific requirements are easily met in terms of the mechanical strength, electrical conductivity and thermal conductivity; however, the main problem to overcome is the susceptibility to corrosion in the acidic environment at elevated temperature (typically 80 °C). Highest corrosion rates are generally found at the anode side of the bipolar plates, where the hydrogen oxidation occurs. At the cathode, side where oxygen reduction takes place at higher potentials, the pH is higher, resulting in lower corrosion rates. The recommended corrosion rate for metal bipolar plates is less than 0.016 mA cm^{-2} [2]. When using metals such as stainless steel, passive oxide layers may form on the metal surface, protecting from corrosion, but at the same time leading to high contact resistance. Therefore, either more noble metals such as titanium or gold have to be used, or when using cheaper metals such as aluminium and stainless steel, these will have to be protected with a corrosion-inhibiting and conductive coating.

---

* Corresponding author. Tel.: +52 999 9813921; fax: +52 999 9813900.
  E-mail address: mascha@cicy.mx (M.A. Smit).

Some stainless steels have been proven to be suitable candidates for bipolar plate material, having low corrosion rates and a stable PEM output [3–6].

Conductive corrosion-inhibiting coatings can be prepared from electroconductive polymers such as polyaniline and polypyrrole. These polymers have high electron conductivity in their oxidated state [7], besides, they have proven to give high corrosion protection to metals such as iron and stainless steel [8–12]. Such conductive polymer coatings can be applied directly by electropolymerization onto the metal substrate, or alternatively, by preparing colloid solutions after chemical polymerization and applying these in paints or sprays. Electropolymerization has the advantage to be a one-step, highly controllable process. In the case of polyaniline however, a highly acidic electrolyte is needed for electropolymerization, making this a less suitable candidate, since there will be a competitive process between electrodeposition and metal oxidation. Polypyrrole though, can be deposited from more neutral solutions.

Pyrrole monomer has been proven to be an effective corrosion inhibitor for stainless steel and aluminium alloys in sulphuric acid solutions [13], while the polymer has been shown to protect from corrosion in different electrolytes [11,12]. The protection mechanism arises from the ability of the doped polymer to successively and reversibly reduce and oxidize, allowing for the metal surface to passivate. This results in protection even for coated damaged surfaces, where the conductive polymer incurs passivity of the exposed metal surface. At high potentials (above the reversible oxidation potential), the polymer will be irreversibly overoxidized and become non-conductive [7].

In this study, we report on the corrosion protection of polypyrrole covered stainless steel SS304, in a simulated PEM fuel cell environment. The coatings were prepared by electrodeposition. Polarization curves are used as an accelerated test to study the corrosion protection at different times of immersion in a wide potential range and SEM allows studying the surface morphology.

2. Experimental

2.1. Electropolymerization

All reactives used in this work are reaction grade materials, the SS304 stainless steel sheet was obtained locally. Electrodes were prepared by cutting stainless steel sheet into pieces of 3 cm × 4 cm, and solding copper wire to one side of these, using standard solding equipment and a drop of phosphoric acid for each electrode to improve adhesion. Samples thus prepared were cleaned in acetone in an ultrasonic bath for 15 min and etched for 1 min in a 10% hydrochloric acid solution at 60 °C, followed by thorough rinsing in distilled water and drying. Using isolation tape, a 1 cm^2 area was selected for exposure, while all other area was carefully covered, avoiding any crevices between tape and substrate. An electrolyte solution was prepared of 0.1 M oxalic acid and 0.1 M pyrrole monomer. In part of the experiments an additional 0.1 M of dodecyl benzene sulphonic acid (DBSA) was added. The prepared electrodes were immersed one by one

as working electrode into the monomer solution. As a reference electrode, a standard calomel electrode (SCE) was used, with platinum wire as auxiliary electrode. Using a Solartron Analytical SI 1287 potentiostat, the polypyrrole was deposited on the substrates by potential cycling between 0 and 900 mV (SCE) at 60 mV s^{-1}, for either 2, 4 or 8 cycles. Prepared samples were rinsed and stored in a dessicator.

2.2. Characterization

Polarization curves were determined after different times of immersion in 0.1 or 0.5 M sulphuric acid at either room temperature or 60 °C. This is considered to be an accelerated test for a simulated PEM fuel cell environment. Prepared samples were immersed for 1, 3 or 24 h in the electrolyte, after which a polarization curve was measured, using a new sample for each curve. Curves were started at 300 mV below open circuit potential, and increased up to 1500 mV, with a current limit of 10 mA cm^{-2}. The scan rate was 1 mV s^{-1}, assumed to be a semi-steady state condition. The potentiostat and electrochemical cell were the same as mentioned above. All potentials referred to are potentials versus the SCE. Scanning electron microscopy was performed at a Philips ESEM 30XL, in BSE mode.

3. Results

3.1. Polymerization

Fig. 1 shows a typical polymerization curve, in this case for 4 deposition cycles. The current density is plotted versus potential in Fig. 1a, and shows that current densities increase rapidly at potentials above 600 mV due to the pyrrole oxidation and subsequent polymerization. At low potentials, small increasing cathodic current densities are due to the reversible reduction of the increasing amount of deposited polymer (followed by its oxidation at anodic potentials). By converting this curve into a current–time plot (Fig. 1b), and integrating to obtain the charge passed during oxidation, the amount of deposited polymer was calculated. For this specific sample, the total charge passed was 0.203 C, corresponding to 1.06 mmol or 0.07 g of polypyrrole. Therefore, for 2, 4 and 8 deposition cycles, the amount of deposited polypyrrole was of the order of 0.04, 0.07 and 0.14 g cm^{-2}, respectively.

3.2. Polarization curves

Polarization curves for bare, cleaned alloy 304 are shown in Fig. 2. All curves show the very similar features. The corrosion potential (or open circuit potential) is close to −500 mV in either or 0.5 M H$_2$SO$_4$ at room temperature, or in 0.1 M H$_2$SO$_4$ at room temperature or at 60 °C. The corrosion current densities can be estimated from these curves based on visually determined Tafel lines and have values between 2 and 20 mA cm^{-2}, the highest values being found for the sample at the elevated temperature of 60 °C. Initial passivation occurs between −400 and −250 mV, with the highest passivation potential for the sample in 0.1 M H$_2$SO$_4$ at 60 °C, followed by the stronger electrolyte of 0.5 M
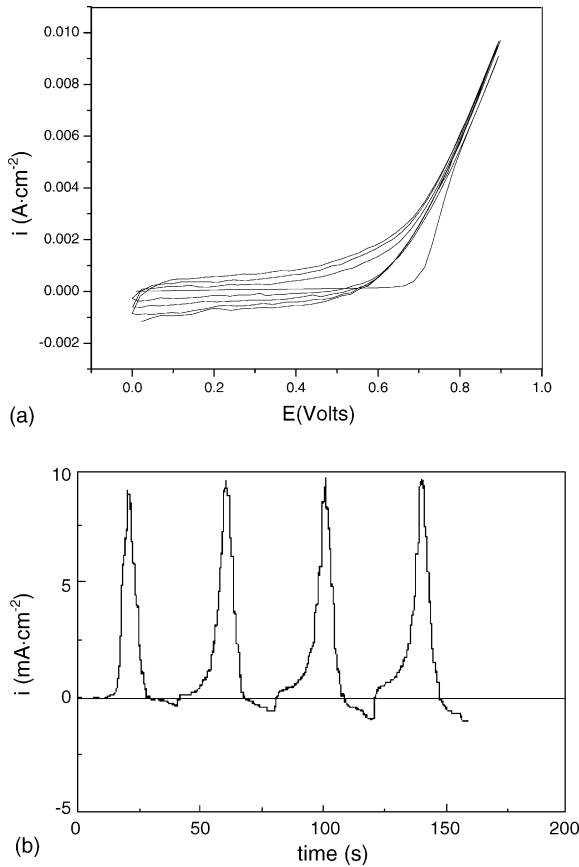
Fig. 1. Typical polymerization curves for polypyrrole on stainless steel SS304 in 0.1 M oxalic acid, with 4 potential cycles between 0 and 900 mV$_{SCE}$ at 1 mV s^{-1}, with (a) potential vs. current density and (b) current density vs. time.
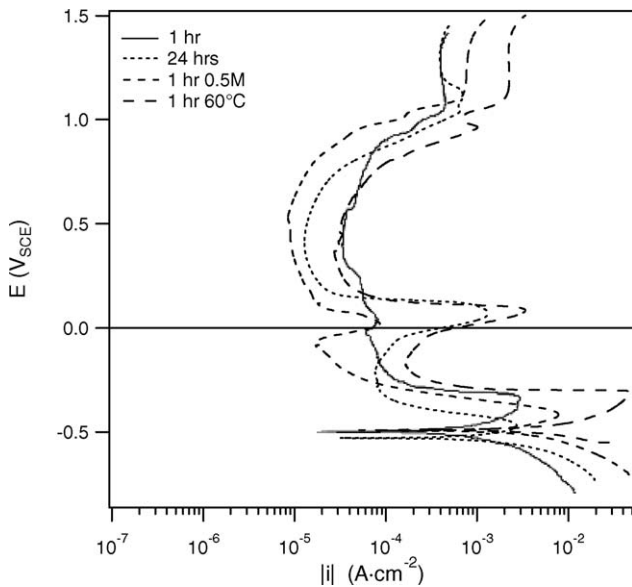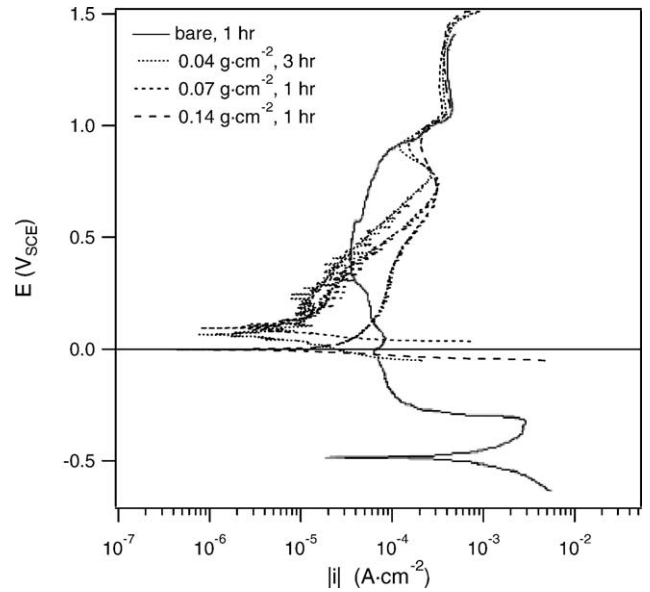

Fig. 3. Polarization curves for coated and uncoated SS304 after short immersion times.

H$_2$SO$_4$. Reactivation is seen around 0 V$_{SCE}$ followed by fast repassivation. The passive current densities range from 10^{-5} to 7×10^{-4} mA cm^{-2} and again are highest for both samples at 1 h immersion (room temperature and 60 °C). Above 500 mV, current densities start to increase slowly, reaching values of about 1 mA cm^{-2} between 900 and 1050 mV. Visual inspection of these samples after testing showed extensive damage and loss of material for the samples tested at 60 °C, even though polarization curves still show repassivation.

For the coated samples, polarization curves in 0.1 M H$_2$SO$_4$ for short immersion times at room temperature can be seen in Fig. 3. For all samples, the presence of the polypyrrole film results in an elevated corrosion potential for short immersion
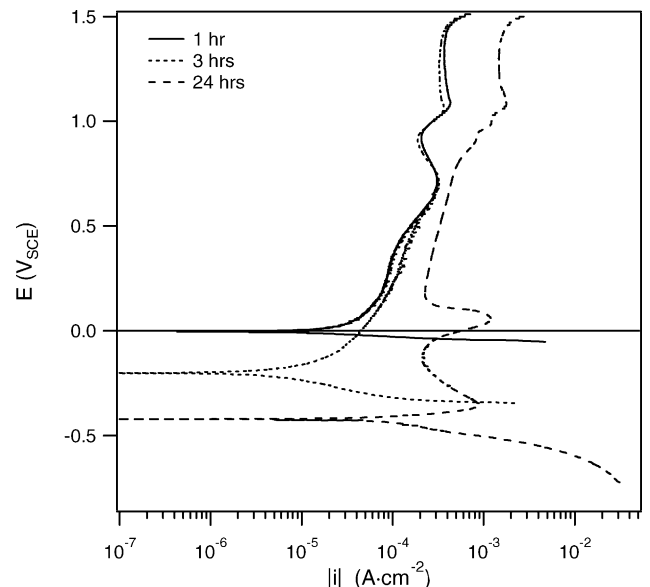

Fig. 2. Polarization curves for bare stainless steel SS304 after immersion in 0.1 M H$_2$SO$_4$ at different conditions: 1 h in 0.1 M sulphuric acid at room temperature (—), 24 h in 0.1 M sulphuric acid at room temperature (···), 1 h in 0.5 M sulphuric acid at room temperature (- - -) and 1 h in 0.1 M sulphuric acid at 60 °C (– –).

Fig. 4. Series of polarization curves for SS304 with 0.14 g cm^{-2} of polypyrrole in 0.1 M H$_2$SO$_4$ at room temperature, after different immersion times.

times. The corrosion current densities have decreased 2 orders of magnitude compared to those for bare alloy, drastically reducing the corrosion rate of the samples. After 1 h immersion, corrosion current densities are 10^{-2} and 3×10^{-2} mA cm^{-2} for the polypyrrole films with 0.07 and 0.14 g cm^{-2}, respectively. Anodic current densities are in the passive range, however the curves show an oxidative peak between 500 and 900 mV, with a maximum at 700 mV, due to the reversible oxidation of the polypyrrole film at this potential. From 900 mV onwards, the current densities increase again, reaching a maximum value of 0.3 mA cm^{-2} at 1050 mV for both curves, being exactly the same value as for bare alloy at equal conditions. At these potentials the reduction of the polypyrrole, as part of the mechanism of protection, is no longer possible. At even higher potentials, the polypyrrole will have overoxidized, and lost its conductivity.

Fig. 4 shows a series of polarization curves at increasing immersion times for samples with 0.14 g cm^{-2} of polypyrrole. With increased immersion times, the corrosion potentials start to decrease, being −200 mV for 3 h immersion and reaching values as for bare alloy after 24 h immersion, indicating that the protective properties of the polypyrrole film are being lost during extended immersion. The same trend was found equally for polypyrrole films deposited from 2, 4 and 8 cycles. Curves at 24 h immersion are very similar to those for bare alloy at 24 h immersion. Effectively, after 24 h immersion, and after running the polarization curve the polymer film was found to fall off of this specific sample.

Fig. 5 shows polarization curves measured after 1 h immersion in 0.1 M H$_2$SO$_4$, at 60 °C. The sample with 0.04 g cm^{-2} of Ppy shows a curve which is again very similar to those obtained for bare alloy, indicating that no protective properties remain for this coating. However, for the films deposited with 0.07 and 0.14 g cm^{-2}, the corrosion current densities were found to have reduced drastically, down to 2×10^{-4} and 3×10^{-3} mA cm^{-2}, well below the recommended maximum
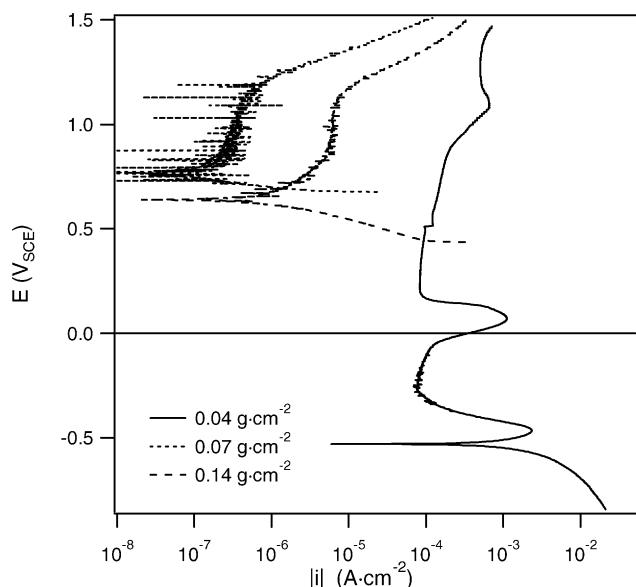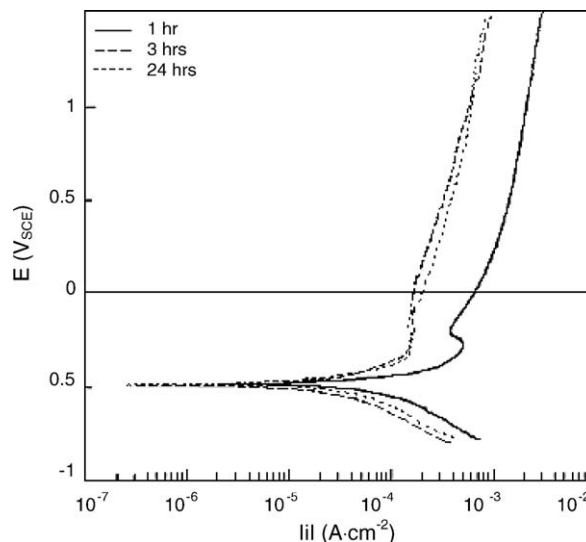

Fig. 6. Series of polarization curves for polypyrrole/DBSA on SS304 in 0.1 M H$_2$SO$_4$ at room temperature.

value [3], and corrosion potentials have increased up to 750 and 650 mV, respectively. The passive current densities are 5×10^{-4} and 7×10^{-3} mA cm^{-2}, respectively, and start to increase at potentials above 1200 and 1100 mV. This means that in the anodic environment of the fuel cell (at positive potentials close to 0 V$_{NHE}$), the samples are in a cathodic state, being completely protected from corrosion.

In order to try to improve the protective properties of the Ppy film, DBSA (dodecyl bencene sulphonic acid) was incorporated into the polymer film. Samples were prepared from an electrolyte of 0.1 M oxalic acid, 0.1 M pyrrole and an additional 0.1 M DBSA, applying 4 polymerization cycles as described before. The polarization curves for these samples are shown in Fig. 6. The corrosion potentials for these samples at immersion times from 1 to 24 h are all −500 mV, being equal to those for bare alloy. Corrosion current densities though, are much
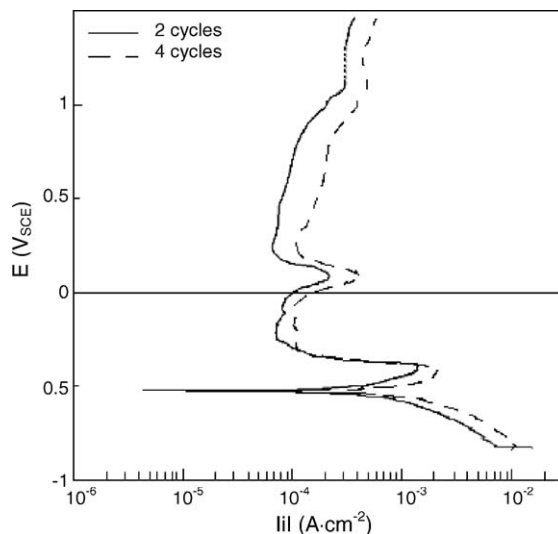

Fig. 5. Polarization curves for 0.04, 0.07 and 0.14 g cm^{-2} of polypyrrole on SS304 after 1 h immersion in 0.1 M H$_2$SO$_4$ at 60 °C.

Fig. 7. Polarization curves for polypyrrole/DBSA on SS304 after 1 h immersion in 0.1 M H$_2$SO$_4$ at 60 °C.

smaller, between 7×10^{-2} and 1×10^{-1} mA cm^{-2}. However, these samples do not show strong passivation as found for the coated samples without DBSA. Therefore, while at potentials just above $0\,V_{SCE}$ the current densities have values similar to those for bare alloy, between 0.1 and 1 mA cm^{-2}, between 150 and 900 mV, current densities are much higher than for bare alloy. At potentials above 1000 mV current densities are again in the same range as those for bare alloy.
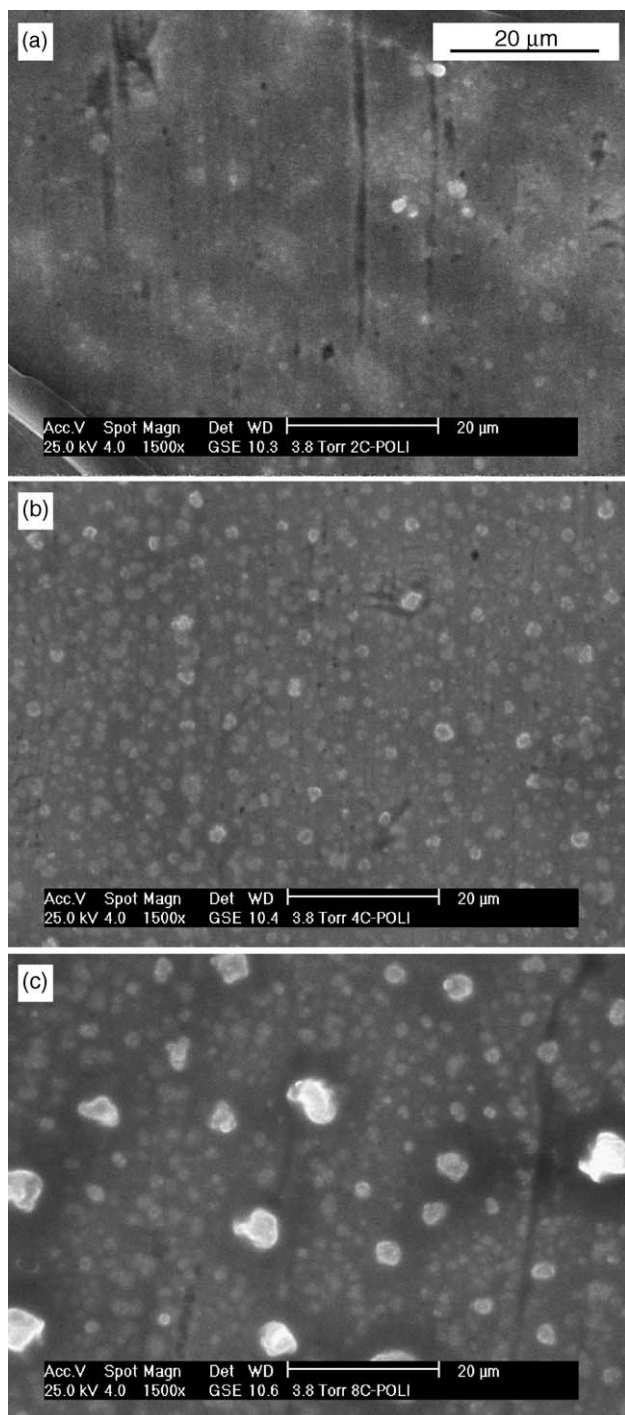
After 1 h in 0.1 M H$_2$SO$_4$ at 60 °C, polarization curves (Fig. 7) show curves as those for bare alloy, indicating a lack of protective properties of the coating.

3.3. SEM

SEM micrographs for the coated samples can be seen in Figs. 8 and 9. Fig. 8 shows samples with 0.04, 0.07 and 0.14 g cm^{-2} of polypyrrole, without the presence of DBSA. For 0.04 g cm^{-2}, the amount of polymer is very small, the substrate features are clearly visible and some larger polymer particles can be seen with a diameter between 1 and 2 µm. For 0.07 g cm^{-2}, the particle size is between 2 and 3 µm, and substrate features are not as clearly visible as for 2 cycles. With 0.14 g cm^{-2} of deposited polypyrrole, a large range of different grain sizes from 2 up to 7 µm can be seen. Large dark areas around some of the larger spheres indicate passivated substrate.

Fig. 9 shows a comparison of samples prepared from an electrolyte with DBSA from 4 deposition cycles and before and after 24 h immersion in 0.1 M sulphuric acid at room temperature. Before immersion (Fig. 9a) the deposited polymer appears more irregular than for the same sample prepared without DBSA (see Fig. 8b), with the polymer spheres being larger, up to 7 µm
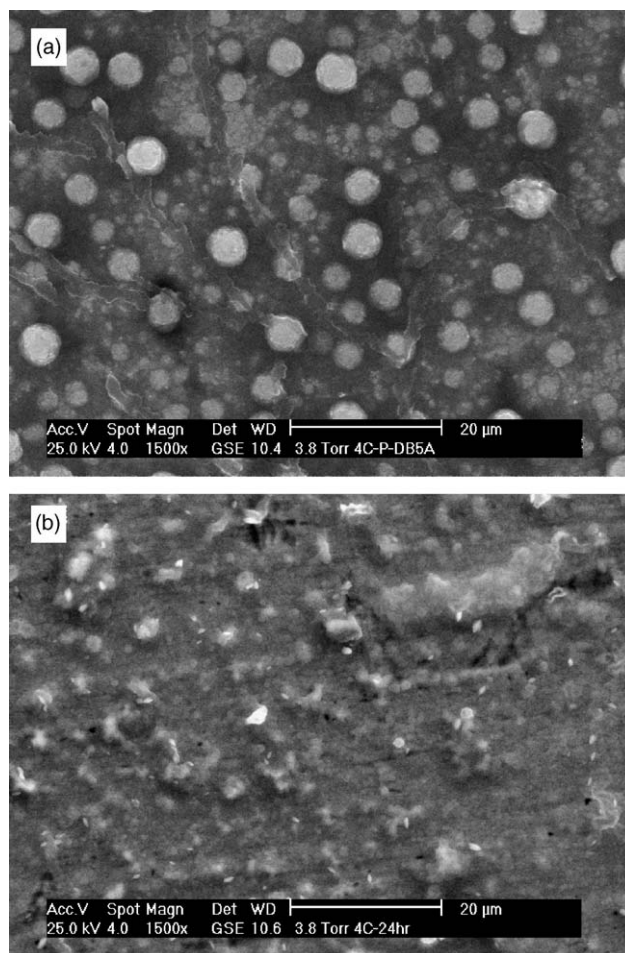

Fig. 8. SEM micrographs for stainless steel with the following polypyrrole coatings: (a) 0.04 g cm^{-2}, (b) 0.07 g cm^{-2} and (c) 0.14 g cm^{-2}.

Fig. 9. SEM micrographs for stainless steel with a polypyrrole-DBSA coating before (a) and after (b) immersion for 24 h in 0.1 M H$_2$SO$_4$ at room temperature.

diameter, and the appearance of channel-like structures not seen in any of the previous samples. This difference may have been caused by the higher acidity of the monomer solution, due to the additional presence of the DBSA. After immersion for 24 h at room temperature and at open circuit conditions (Fig. 9b), the polymer coating has virtually disappeared, only some small particles appear to have been left on the surface, and the surface has a cloudy appearance, different from bare alloy. From the polarization curves reported above, it is known that the corrosion current densities are still 1 order smaller than those for bare samples at the same conditions, indicating that some protective properties do remain present. The polypyrrole may have been incorporated into a protective oxide film.

4. Conclusions

Polypyrrole coatings 0.04, 0.07 and 0.14 g cm^{-2} (2, 4 and 8 deposition cycles, respectively) were electropolymerized onto stainless steel SS304. Polarization curves taken after immersion in a simulated PEM fuel cell environment, show that these coatings are capable of passivating the samples surface and reducing the corrosion current densities up to 4 orders of magnitude at free corrosion potentials. Oxidation rates at PEM anode potentials were also reduced by several orders of magnitude. However, the protective properties are being lost with increasing time of immersion. Therefore, although the polypyrrole coating can greatly reduce corrosion rates for stainless steel bipolar plates, the specific coating composition will need to be modified in order to maintain protective properties for long fuel cell lifetimes. It was intended to improve coating properties by the addition of DBSA and it was shown that this leads to lower corrosion current densities compared to bare metal, though not as low as for the samples coated with polypyrrole without the incorporation of DBSA. However, at fuel cell conditions, current densities are equal or much larger as for bare metal, due to a loss of passivity of the metal surface.

SEM micrographs were used to study the coating morphology. A typical grain structure was found for all coatings.

The grain size increases with increasing amount of deposited polypyrrole. The most homogeneous film was found for the film with 0.07 g cm^{-2} of polypyrrole. The inclusion of DBSA leads to a change in morphology, with larger grain size and the appearance of channel-like structures. Immersion for 24 h in 0.1 M sulphuric acid at room temperature and at open circuit conditions, led to a change in surface morphology, with the polymer particles apparently incorporated into a metal oxide film.

Acknowledgements

References

[1] A. Hermann, T. Chaudhuri, P. Spagnol, Int. J. Hydrogen Energy 30 (12) (2005) 1297–1302.
[2] V. Mehta, J.S. Cooper, J. Power Sources 114 (2003) 32–53.
[3] R.C. Makkus, A.H.H. Janssen, F.A. de Bruijn, R.K.A.M. Mallant, J. Power Sources 86 (2000) 274–282.
[4] D.P. Davies, P.L. Adcock, M. Turpin, S.J. Rowen, J. Power Sources 86 (2000) 237–242.
[5] J. Wind, R. Späh, W. Kaiser, G. Böhm, J. Power Sources 105 (2002) 256–260.
[6] H. Wang, J.A. Turner, J. Power Sources 128 (2004) 193–200.
[7] T.A. Skotheim, R.L. Elsenbauer, J.R. Reynolds (Eds.), Handbook of Conducting Polymers, second ed., Marcel Dekker, New York, 1998.
[8] D.W. DeBerry, J. Electrochem. Soc. 132 (1985) 132.
[9] B. Wessling, Adv. Mater. 6 (1994) 226.
[10] B.N. Grgur, N.V. Krstajić, M.V. Vojnović, Č. Lačnjevac, Lj. Gajić-Krstajić, Progr. Org. Coat. 33 (1998) 1–6.
[11] P. Herrasti, P. Ocón, Appl. Surf. Sci. 172 (2001) 276–284.
[12] A.A. Hermas, M. Nakayama, K. Ogura, Electrochim. Acta 50 (2005) 3640–3647.
[13] R.M. Hudson, C.J. Warning, Met. Finish. 64 (1966) 63.